

On justification of Cu(II) environment in mononuclear complexes: Joint X-ray and AIM studies

Alexandr Fonari^{a,*}, Evgeniya S. Leonova^{a,b}, Mikhail Yu. Antipin^{a,b}

^aNew Mexico Highlands University, Las Vegas, NM 87701, USA

^bA.N. Nesmeyanov Institute of Organoelement Compounds, Russian Academy of Sciences, Vavilova str. 28, 119991 Moscow, Russian Federation

ARTICLE INFO

Article history:

Received 11 January 2011

Accepted 4 April 2011

Available online 12 April 2011

Keywords:

Cu(II) square-planar geometry

Extended H-bonding system

X-ray

Quantum theory of atoms in molecules

ABSTRACT

Interaction of copper(II) acetate with benzoic acid (benzene-1,3,5-tricarboxylic acid = H₃-btc and 3,5-dinitro-benzoic acid = H-dnb) and pyridine (Py) resulted in two mononuclear square-planar complexes with the compositions [Cu(H₂-btc)₂(Py)₂] (**1**) and [Cu(dnb)₂(Py)₂] (**2**). The recrystallization of **2** from dimethylsulfoxide (DMSO) yielded the square-bipyramidal complex [Cu(dnb)₂(DMSO)₂(H₂O)₂] (**3**). Crystal structures of **1–3** were determined by single crystal X-ray diffraction at 100 K. The square-planar Cu(II) geometry with the Cu–O and Cu–N distances of 1.924(2), 1.925(2) and 2.024(3) and 2.025(3) Å in **1**, and 1.930(4) and 2.033(5) Å in **2** was found. The extended H-bonding system in **1** built on the robust carboxylic synthons is giving rise to the high-ordered porous layered structure. Insight into metal center environment and stabilizing intramolecular short interactions is obtained through quantum theory of atoms in molecules (QTAIM). As revealed by QTAIM, in octahedral complex **3** Cu–dnb and Cu–DMSO bonds are stronger than Cu–N bonds in **1** and **2**.

© 2011 Elsevier Ltd. All rights reserved.

1. Introduction

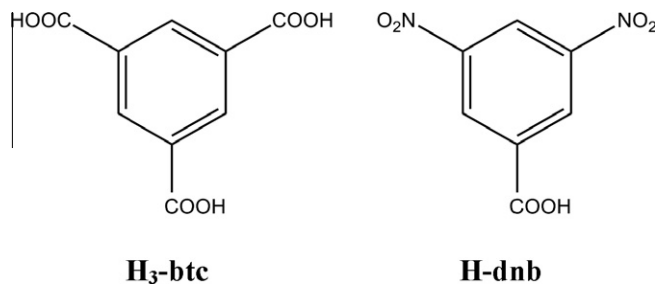
Metal–organic building blocks as a prototype to highly porous metal–organic frameworks [1] continue to be an active research field because of the large variety of metal–ligand combinations. The d⁹ configuration of the Cu(II) cation favors either a square-planar, square-pyramidal or square-bipyramidal geometries. Mono- and polycarboxylic acids are by far the most widely used organic ligands for the synthesis and crystal engineering of compounds that exhibit highly ordered 2D or 3D networks. Among them benzene-1,3,5-tricarboxylic acid (H₃-btc, also known as trimesic acid) occupies a special place, as it is a polyfunctional carboxylic acid with 3-fold symmetry comprising a phenyl ring and three identical carboxyl end groups in the same plane [2]. Starting from the seminal *Science* paper [3] which reported a highly porous metal coordination polymer [Cu₃(btc)₂(H₂O)₃]_n various open frameworks with the fascinating supramolecular architectures containing Cu(II) as a metal center and polycarboxylic aromatic acids as linkers were described. In particular, benzene-1,3,5-tricarboxylic acid was explored either as a unique ligand for construction of Cu(II)-based carboxylate networks [4] or in combination with different amines as auxiliary ligands [5]. Along with H₃-btc, its nitro- and dinitro-analogs with the same positions of the substituents in the aromatic core, have been successfully applied so far for

* Corresponding author. Tel.: +1 5056522245.

E-mail addresses: alexandr.fonari@gmail.com (A. Fonari), mishan@nmhu.edu (M.Yu. Antipin).

generation of multinuclear and polymeric Cu(II)-carboxylic networks [6]. The diversity of the networks built from the similar components and explained by the possibility of different coordination environment of Cu(II), different modes of carboxylic groups coordination, and different degree of deprotonation of starting acid was found using X-ray analysis of the structure of such compounds. An additional insight into metal center environment can be obtained through quantum theory of atoms in molecules (QTAIM).

The topological analysis, based on the QTAIM [7,8], is a useful tool to justify the metal coordination environment as well as to estimate the stabilizing impact of short intramolecular interactions in such complexes. Recently a number of papers describing different bonding aspects of pure organic molecules as well as coordination complexes were published using QTAIM approach. Analysis of the local electron density properties at bond critical points (BCPs) allows qualitative and quantitative classification of the metal–ligand bonds. Using this approach Firme et al. compared the stability of the titanium complexes based on the number of BCPs found between metal and ligands [9]. Cukrowski and co-workers estimated the stabilizing effect of H···H close contacts in Zn(II) and Ni(II) complexes [10]. As the correct assignment of the primary coordination sphere for Cu(II) still remains a challenge [11,12] the modern computational approaches such as QTAIM demonstrate their facilities in solving this problem. For example, consideration of a number of topological indicators by Farrugia with co-workers for Cu(II) 3-amino-propanolato complexes containing weakly coordinated anions provided an insight into the differing electrostatic and covalent contributions to the chemical bonds



Scheme 1.

[13], while Robertazzi et al. successfully employed QTAIM calculations on copper phenanthroline complexes to show the decrease in strength of Cu–N bond when water molecule is included into copper coordination [14].

With the aim to study the electron density topology of the Cu-center environment we fulfilled the synthesis of two novel

Table 3

Intermolecular hydrogen bonding in 1–3. Distances are in (Å) and angles in (°).

D–H...A	d(D–H)	d(H...A)	d(D...A)	∠DHA
Compound 1				
C(7)–H(7A)...O(9) ^{#1}	0.95	2.27	3.184(4)	162
C(19)–H(19A)...O(3) ^{#2}	0.95	2.28	3.200(4)	163
O(3)–H(3)...O(8) ^{#1}	0.81(2)	1.89(2)	2.671(3)	165(5)
O(6)–H(6)...O(11) ^{#3}	0.97(7)	1.65(7)	2.605(3)	165(7)
O(9)–H(9)...O(2) ^{#2}	0.82(5)	1.86(5)	2.663(4)	169(5)
O(12)–H(12)...O(5) ^{#4}	0.81(2)	1.97(8)	2.628(3)	137(11)
Compound 2				
C(11)–H(11A)...O(2) ^{#5}	0.95	2.57	3.206(8)	124
C(11')–H(11B)...O(2') ^{#6}	0.95	2.54	3.164(8)	123
C(9')–H(9'A)...O(3) ^{#1}	0.95	2.51	3.145(8)	124
Compound 3				
O(1w)–H(1w)...O(2)	0.84(3)	1.83(3)	2.617(2)	156(2)
O(2w)–H(2w)...O(7) ^{#7}	0.75(3)	1.99(3)	2.724(2)	167(3)

Symmetry transformation used to generate equivalent atoms: #1 = 1 + x, y, z; #2 = x – 1, y, z; #3 = 1 + x, y, 1 + z; #4 = x – 1, y, z – 1; #5 = –1 – x, 1 – y, –z; #6 = 1 – x, –y, 1 – z; #7 = –x, –y, –z.

Table 1

Selected crystal data, details of data collection and structure refinement for 1–3.

Compound	1	2	3
Empirical formula	C ₂₈ H ₂₀ CuN ₂ O ₁₂	C ₂₄ H ₁₆ CuN ₆ O ₁₂	C ₁₈ H ₂₂ CuN ₄ O ₁₆ S ₂
Formula weight	640.00	643.97	678.06
T (K)	100(2)	100(2)	100(2)
Crystal system	monoclinic	triclinic	monoclinic
Space group	P2 ₁ /c	P1	P2 ₁ /n
a (Å)	12.9247(10)	5.5818(13)	10.6242(14)
b (Å)	13.9421(11)	10.327(2)	5.2823(6)
c (Å)	16.8693(10)	21.550(5)	22.573(3)
α (°)	90	86.350(4)	90
β (°)	114.691(4)	87.059(4)	91.932(4)
γ (°)	90	89.504(4)	90
V (Å ³)	2761.9(3)	1238.0(5)	1266.1(3)
Z	4	2	2
D _{calc} (g cm ^{–3})	1.539	1.727	1.779
μ (mm ^{–1})	0.861	0.965	1.116
F(0 0 0)	1308	654	694
Reflections collected/unique	32073/4869	4344/4344	5634/2218
Data/restraints/parameters	4869/2/414	4344/0/392	2218/0/197
Goodness-of-fit on F ²	0.976	1.120	1.050
R ₁ , wR ₂ (I > 2σ(I))	0.0407, 0.0995	0.0678, 0.1940	0.0252, 0.0639
R ₁ , wR ₂ (all data)	0.0704, 0.1201	0.0803, 0.2034	0.0295, 0.0666

Table 2

Selected experimental and calculated geometric parameters of the described structures. Distances are in (Å) and angles in (°).

Parameters	1	1c	2	2'	2c ^a	3	3c ^{a,b}
Cu(1)–O(1)	1.924(2)	1.987	1.930(4)	1.934(4)	1.994	1.968(1)	1.988
Cu(1)...O(2)	2.900(2)	2.596	3.001(5)	2.796(5)	2.604	3.298(2)	3.283
Cu(1)–O(7)	1.925(2)	1.987	–	–	1.994	2.371(1)	1.988
Cu(1)...O(8)	2.929(2)	2.596	–	–	2.604	–	3.283
Cu(1)–O(1w)	–	–	–	–	–	1.971(2)	2.071
Cu(1)–N(1)	2.025(3)	2.080	2.033(5)	2.042(5)	2.068	–	–
Cu(1)–N(2)	2.024(3)	2.080	–	–	2.068	–	–
C(1)–O(1)	1.283(4)	1.300	1.285(8)	1.272(8)	1.296	1.269(2)	–
C(1)–O(2)	1.231(4)	1.240	1.223(8)	1.228(8)	1.239	1.243(2)	–
C(13)–O(7)	1.275(4)	1.300	–	–	1.296	–	–
C(13)–O(8)	1.245(4)	1.240	–	–	1.239	–	–
O(1)–Cu(1)–O(7)	–	–	–	–	–	93.4(1)	90.8
O(1)–Cu(1)–O(1w)	–	–	–	–	–	92.8(1)	93.3
O(7)–Cu(1)–O(1w)	–	–	–	–	–	87.7(1)	86.1
O(1)–Cu(1)–N(1)	89.7(1)	90.0	90.9(2)	90.2(2)	90.0	–	–
O(1)–Cu(1)–N(2)	90.3(1)	90.0	–	–	90.0	–	–
O(7)–Cu(1)–N(1)	90.0(1)	90.0	–	–	90.0	–	–
O(7)–Cu(1)–N(2)	90.0(1)	90.0	–	–	90.0	–	–

^a When possible, same labeling convention as in 1 is obeyed.

^b Due to inversion center pseudosymmetry only half of the molecular geometry is listed.

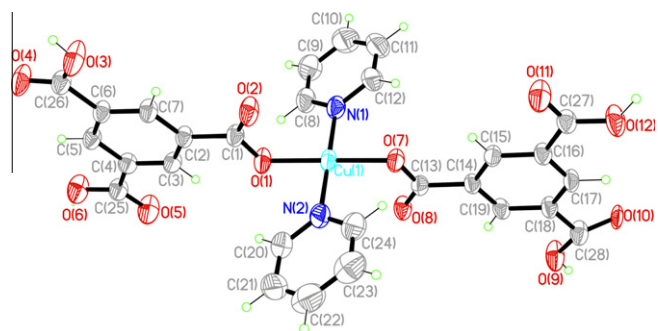


Fig. 1. ORTEP plot of **1** with the numbering scheme. Thermal ellipsoids are shown with the 50% probability level. The major position is shown for the disordered O(10) atom.

Cu(II)-carboxylate complexes, $[\text{Cu}(\text{H}_2\text{-btc})_2(\text{Py})_2]$ (**1**) and $[\text{Cu}(\text{dnb})_2(\text{Py})_2]$ (**2**) obtained by the reaction of copper(II) acetate with pyridine, and two geometrically similar benzoic acids, benzene-1,3,5-tricarboxylic acid ($\text{H}_3\text{-btc}$), and 3,5-dinitro-benzoic acid (H-dnb) (Scheme 1). Complex $[\text{Cu}(\text{dnb})_2(\text{DMSO})_2(\text{H}_2\text{O})_2]$ (**3**) previously reported as a product of interaction of copper sulfate with 3,5-dinitrobenzoate of piperidine in DMSO [15] was obtained by recrystallization of **2** from DMSO. The low temperature single crystal X-ray study along with the comparative QTAIM evaluation for **1–3** is reported herein.

1.1. Synthesis

Compounds **1** and **2** were obtained following the synthetic procedure described in [16] by mixing of copper acetate monohydrate,

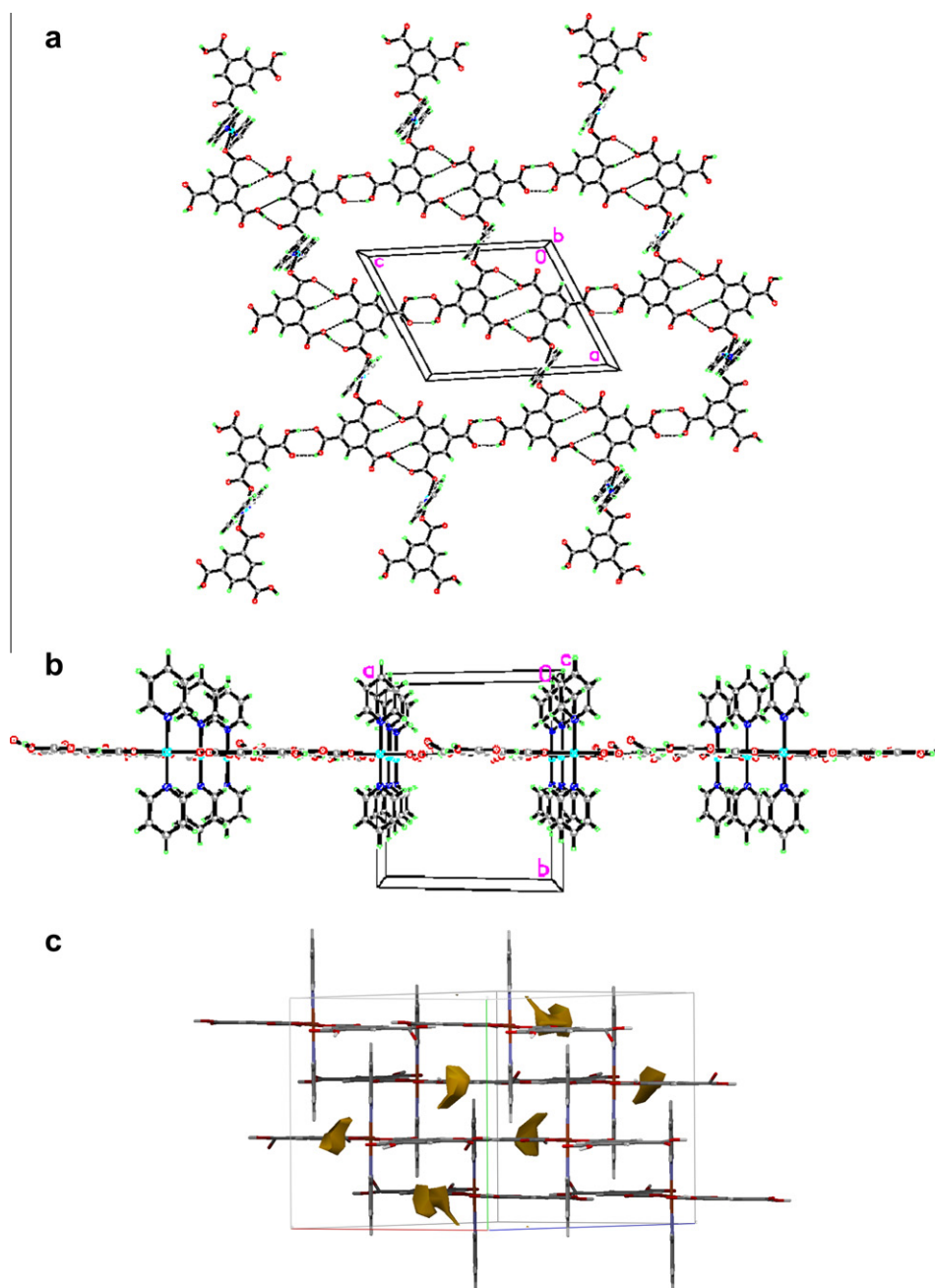


Fig. 2. H-bonded layer in **1** viewed along *b* (a) and *c* (b) axes; crystal packing with the voids shown in brown (c). (For interpretation of the references to colour in this figure legend, the reader is referred to the web version of this article.)

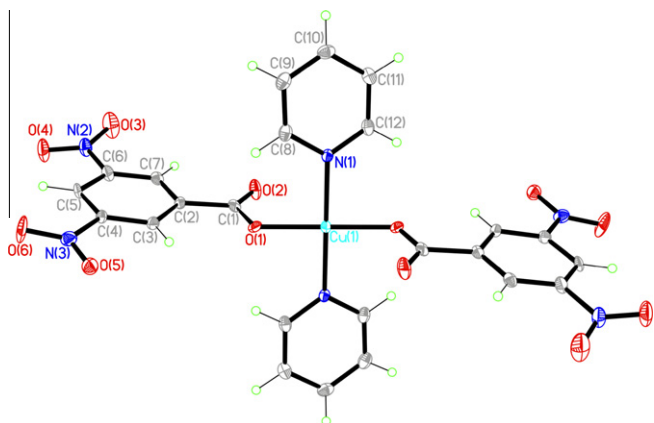


Fig. 3. ORTEP plot of **2** with the numbering scheme. Thermal ellipsoids are shown with the 50% probability level.

pyridine, and corresponding acid in anhydrous methanol. In both cases, light blue plate-like crystals suitable for single crystal X-ray analysis were found upon evaporation. Crystals of **3** were obtained upon recrystallization of **2** from aqueous DMSO.

1.2. X-ray investigations

Single crystal X-ray diffraction experiments for **1–3** were carried out with a Bruker SMART APEX II diffractometer with CCD area detector (graphite monochromated Mo K α radiation, $\lambda = 0.71073$ Å), ω -scans with a 0.5° step in ω at 100 K. Semi empirical method S_{AD}ABS [17] was applied for absorption correction for all three compounds. Compound **2** was pseudomerohedrally twinned. By running the TWINROT program within the PLATON [18] package the twinned matrix $(-1\ 0\ 0\ 0\ 1\ 0\ 0\ 0\ -1)$ was obtained for the minor component (38%). From the total number of 4350 reflections 750 were removed from the *hkl* file and SHELX HKLF 5 format file was generated for the refinement. The structure solution and refinement preceded similarly using SHELX-97 program package for all structures [19]. The structures were solved by direct methods and refined by the full-matrix least-squares technique against F^2 with the anisotropic temperature parameters for all non-hydrogen atoms. The hydrogen atoms on the carboxylic groups in **1**, and in water molecule in **3** were located from the Fourier electron density map and refined isotropically. All C-bound hydrogen atoms were refined within the riding model. Data reduction and further calculations were performed using Bruker SAINT+ and SHELXTL NT [19] program packages. The X-ray data and details of the refinement for **1–3** are summarized in Table 1, the selected geometric parameters are given in Table 2, the hydrogen bonding geometry is given in Table 3.

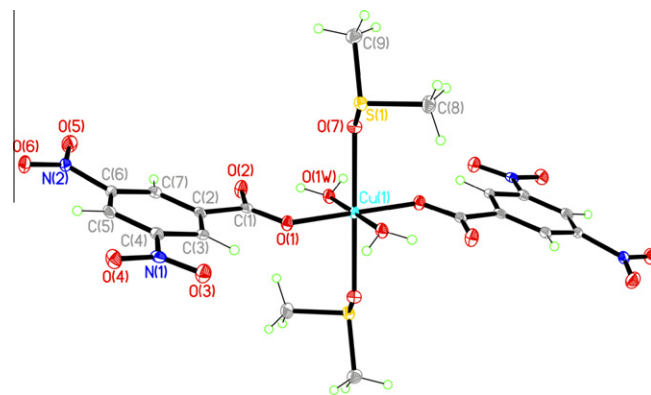


Fig. 5. ORTEP plot of **3** with the numbering scheme. Thermal ellipsoids are shown with the 50% probability level.

1.3. Computational methodology

All calculations were carried without any symmetry restriction in the doublet ground state, for isolated molecule, using the GAUSSIAN09 program [20]. Geometry optimizations were performed using B3LYP [21–23] functional and 6-31G** basis set for C, H, N and O atoms, and effective core potential basis set LANL2DZ for Cu atom [24] (tail c is added for calculated structures). Single point energies were calculated in gas phase starting from optimized geometries at the B3LYP/6-31++G** level of theory for all atoms. Resulting wave functions were used for further studies of the electron density using topological approach of the QTAIM with AIMALL (Version 10.12.08) [25].

2. Results and discussion

2.1. X-ray structures

X-ray structural analysis revealed that complexes **1** and **2**, in contrast with previously published results [16], where authors used the similar synthetic procedure, do not contain water molecules in Cu coordination sphere. Complex $[\text{Cu}(\text{H}_2\text{-btc})_2(\text{Py})_2]$ (**1**) crystallizes in the monoclinic centrosymmetric $P2_1/c$ space group with an entire molecule in the asymmetric unit (Fig. 1). The Cu(II) center adopts a square-planar geometry by coordinating to two pyridine molecules in *trans*-position at Cu–N distances of 2.024(3) and 2.025(3) Å, and two *trans*-carboxylate O atoms of two monodeprotonated $(\text{H}_2\text{-btc})^-$ ligands, at C–O distances of 1.924(2) and 1.925(2) Å with *cis*-angles ranging from 89.7(1) to 90.3(1)° for the metal center (Table 2).

Trans-coordinated ligands are arranged essentially in the same planes, the dihedral angle between the average planes through the Py molecules is equal to 0.5(2)°, and between two $\text{H}_2\text{-btc}$

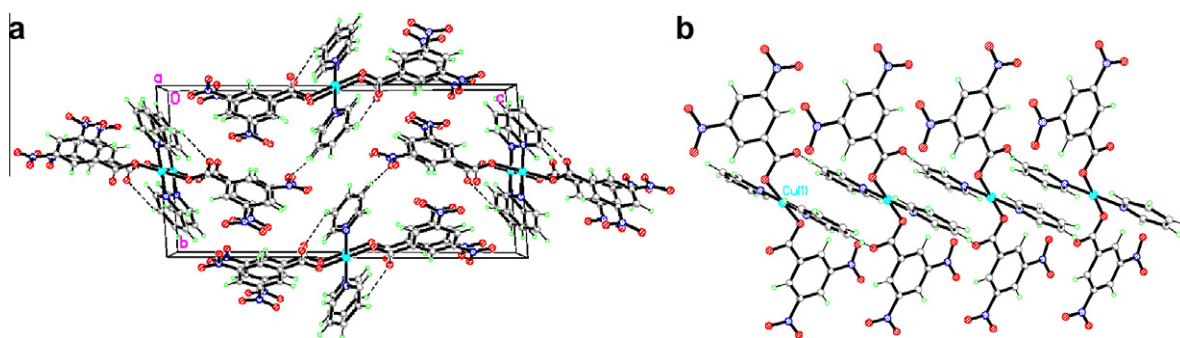


Fig. 4. Crystal packing of **2** viewed along *a*-axis (a) one stack held by weak hydrogen bonds (b).

moieties is equal to $3.3(1)^\circ$. So, the mutual arrangement of the distinctive ligands which are almost perpendicular can be characterized by two, practically planar fragments, plane P_A that includes all non-H atoms from two H_2 -btc residues, (excluding the disordered O(10) atom), and plane P_B that contains two pyridine molecules, dihedral angle P_A/P_B being equal to $89.2(1)^\circ$.

It was reported that free H_3 -btc assembles in diverse supramolecular structures due to the trigonal exodentate functionality, and the most common motif is a planar honeycomb network structure formed through the dimerization of the carboxyl groups [2]. The reported examples reveal different degree of H_3 -btc deprotonation

in the Cu(II)-based networks, where the hydrogen bonds arising from the COOH carboxylic groups contribute to the structure robustness [26]. In **1**, each of two $(H_2$ -btc) $^-$ anions use only one carboxylate group for the monodentate coordination to the Cu(II) center. Four other carboxylic groups generate the planar extended system of hydrogen bonding parallel to the (0 1 0) plane, built on the robust $R_8^8(8)$ and $R_8^8(16)$ carboxylic patterns [27], the latter represents the combination of three shared molecular patterns, $R_2^2(7)$, $R_2^2(10)$, $R_2^2(7)$ (Table 3). These interactions acting in the concerted way result into honeycomb network with the $8.6 \times 16.9 \text{ \AA}$ cavities (Fig. 2a) partially filled by the pillared Py molecules from adjacent

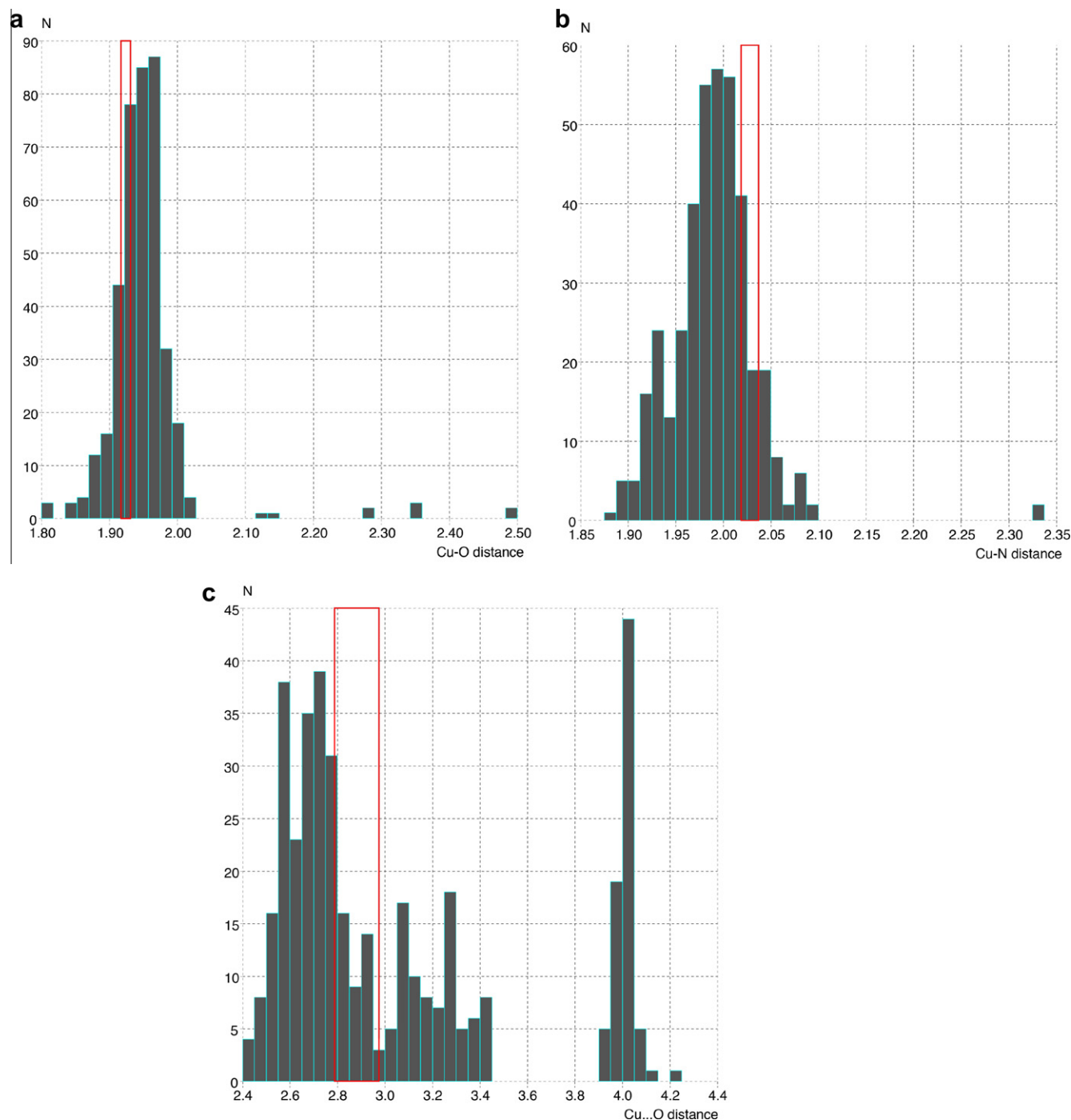


Fig. 6. Bond length distribution in four-coordinated Cu(II) environment: Cu–O coordination bonds (a); Cu–N coordination bonds (b); Cu...O non-coordination distances (c); All distances are given in Å. Red rectangle marks range of the bond lengths in **1** and **2**. (For interpretation of the references to colour in this figure legend, the reader is referred to the web version of this article.)

Table 4

Topological properties of the electron density (ρ) at the selected BCPs: Laplacian of the electron density ($\nabla^2\rho_{\text{BCP}}$), total energy density (H), kinetic energy density (G) and the potential energy density (V). Densities are measured in $\text{e}\text{\AA}^{-3}$, Laplacian of the electron density in $\text{e}\text{\AA}^{-5}$ and energies in Hartree \AA^{-3} . Refer to the ORTEP plots for the labeling convention.

Bond	ρ			$\nabla^2\rho$			H			G			V		
	1c	2c	3c	1c	2c	3c	1c	2c	3c	1c	2c	3c	1c	2c	3c
Cu(1)–O(1)	0.084	0.083	0.084	0.322	0.314	0.370	–0.028	–0.028	–0.025	0.109	0.106	0.118	–0.137	–0.134	–0.144
Cu(1)–O(7)	0.084	0.083	0.084	0.322	0.314	0.370	–0.028	–0.028	–0.025	0.109	0.106	0.118	–0.137	–0.134	–0.144
Cu(1)–N(1)	0.076	0.078	–	0.228	0.235	–	–0.028	–0.030	–	0.085	0.088	–	–0.113	–0.118	–
Cu(1)–N(2)	0.076	0.078	–	0.228	0.235	–	–0.028	–0.030	–	0.085	0.088	–	–0.113	–0.118	–
Cu(1)–O(1w)	–	–	0.076	–	–	0.305	–	–	–0.024	–	–	0.100	–	–	–0.124
Cu(1)–O(1') ^a	–	–	0.084	–	–	0.370	–	–	–0.026	–	–	0.118	–	–	–0.144
Cu(1)–O(7')	–	–	0.084	–	–	0.370	–	–	–0.026	–	–	0.118	–	–	–0.144
Cu(1)–O(1w')	–	–	0.076	–	–	0.305	–	–	–0.024	–	–	0.100	–	–	–0.124

^a Related by inversion center pseudosymmetry.

layers. The partially interdigitated layers are packed with the generation of small voids (40\AA^3) (Fig. 2b and c) [18].

Complex $[\text{Cu}(\text{dnb})_2(\text{Py})_2]$ (**2**) crystallizes in the triclinic centrosymmetric $P\bar{1}$ space group with two symmetrically independent complexes (**2** and **2'**) in the asymmetric unit. Both of them reside on inversion centers, with structural parameters similar to those in **1** (Fig. 3 depicts complex **2**). In both complexes the centrosymmetric N_2O_2 -coordination core is formulated by two dnb residues that coordinate in a monodentate mode, Cu(1)–O(1) 1.930(4) \AA in **2** and 1.934(4) \AA in **2'**, and two molecules of pyridine, Cu(1)–N(1) being 2.032(5) \AA in **2**, and 2.042(5) \AA in **2'**. The O(2) atom evidently does not coordinate to the metal center, as suggested by long Cu(1)–O(2) separations in both complexes, and differentiated C–O distances for the coordinated and non-coordinated oxygen atoms in carboxylic groups. The regular square-planar geometry of the metal center is supported by the practically equal N–Cu(1)–O *syn*-angles close to 90° (Table 2). The similar square-planar Cu(II) geometry has been registered for example in *trans*-bis(2-amino-5-methyl-1,3,4-thiadiazole-*N*)-bis(3,5-dicarboxybenzoato-*O*)-copper(II) [26a], and *catena*-[bis(μ_2 -5-nitroisophthalato)-tetrakis(benzimidazole)-di-copper] [28].

The dnb residues are characterized by the planar skeletons with the carboxylic and nitro-groups being practically coplanar with the aromatic core. The dihedral angle P_A/P_B is equal to $70.6(1)^\circ$ in **2** being somewhat smaller than $81.0(1)^\circ$ in **2'** (as for **1**, P_B contains atoms from pyridine molecule).

In the crystal, complexes **2** and **2'** generate uniform chains (Fig. 4) along the shortest crystallographic *a*-axis (Table 1) with the parallel alignment of Py and dnb moieties, and held by similar weak hydrogen bonds with involvement of O(2) oxygen atom of carboxylic groups, C(11)–H(11A)···O(2) ($-1-x, 1-y, -z$) 3.205(8) \AA for **2**, and C(11')–H(11A)···O(2')(1-x, -y, 1-z) 3.164(8) \AA for **2'** (Fig. 4). The chains are held *via* C(9')–H(9'A)···O(3)(1+x, y, z) 3.146(8) \AA interactions with participation of nitro group as H-bond acceptor. All these weak hydrogen bonds are in the range of H···O standard distances (Table 3) [29].

The recrystallization of **2** from DMSO yielded the square-bipyramidal complex $[\text{Cu}(\text{dnb})_2(\text{DMSO})_2(\text{H}_2\text{O})_2]$ (**3**) with the substitution of two Py molecules by four solvate species including two water and two DMSO molecules. Complex **3** resides on the center of symmetry (Fig. 5). Two dnb residues, and two water molecules are displayed in the equatorial plane, Cu–O(carboxyl) = 1.968(1), and Cu–O(H_2O) = 1.971(2) \AA , while two DMSO molecules occupy the axial positions, Cu–O(DMSO) = 2.371(1) \AA . The distribution of distances related to metal–ligand interactions in **3** is similar to **1** and **2** and may serve as an additional proof for monodentate mode of carboxylic group coordination in **1** and **2**. The decrease of the unit cell volume in **3** by 60\AA^3 was observed, comparing to the room temperature experiment reported in [15].

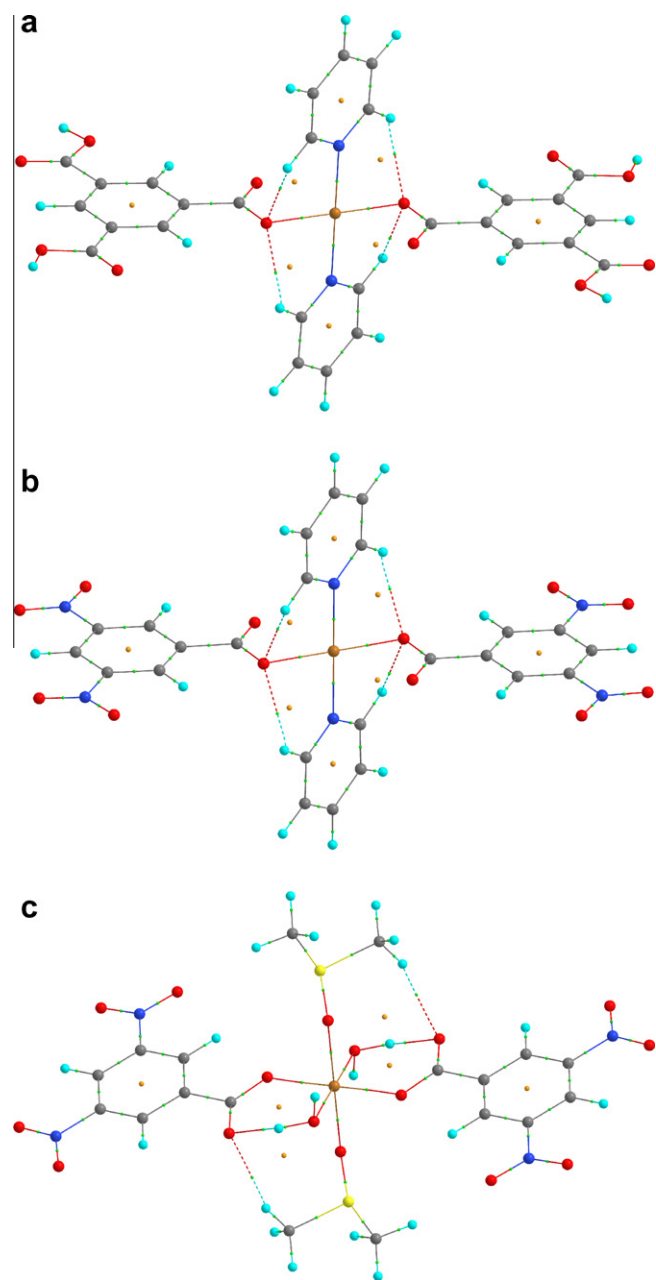


Fig. 7. Molecular graph of **1c** (a), **2c** (b) and **3c** (c) showing C–H···O bond paths with dashed lines. Bond critical points (BCPs) are marked with small green spheres, ring critical points (RCPs) are marked with small orange spheres. (For interpretation of the references to colour in this figure legend, the reader is referred to the web version of this article.)

Table 5
Structural and nonstructural rings revealed by QTAIM. Densities are measured in $\text{e} \text{Å}^{-3}$, Laplacian of the electron density in $\text{e} \text{Å}^{-5}$. Refer to the ORTEP plots for the labeling convention.

Rings	ρ			$\nabla^2 \rho_{\text{BCP}}$		
	1c	2c	3c	1c	2c	3c
C(2)–C(3)–C(4)–C(5)–C(6)–C(7)	0.021	0.021	0.021	0.161	0.162	0.162
C(14)–C(15)–C(16)–C(17)–C(18)–C(19)	0.021	0.021	0.021	0.161	0.162	0.162
N(1)–C(8)–C(9)–C(10)–C(11)–C(12)	0.022	0.022	–	0.175	0.175	–
N(2)–C(20)–C(21)–C(22)–C(23)–C(24)	0.022	0.022	–	0.175	0.175	–
Cu(1)–N(1)–C(8)–H(8)–O(1)	0.011	0.011	–	0.054	0.052	–
Cu(1)–N(1)–C(12)–H(12)–O(7)	0.011	0.011	–	0.054	0.052	–
Cu(1)–N(2)–C(20)–H(20)–O(1)	0.011	0.011	–	0.054	0.052	–
Cu(1)–N(2)–C(24)–H(24)–O(7)	0.011	0.011	–	0.054	0.052	–
Cu(1)–O(1w)–H(1w)–O(2)–C(1)–O(1)	–	–	0.014	–	–	0.064
Cu(1)–O(1w')–H(1w')–O(2')–C(1')–O(1')	–	–	0.014	–	–	0.064
Cu(1)–O(7)–S(1)–C(8)–H(8c)–O(2')	–	–	0.003	–	–	0.011
Cu(1)–O(7')–S(1')–C(8')–H(8c')–O(2)	–	–	0.003	–	–	0.011

The bond lengths distribution in the metal coordination core for four-coordinated Cu(II) compounds that include aromatic carboxylic group and N-base as coordinating species, has been augmented using the CSD data [30]. The CSD search (CSD version 5.31) resulted in 159 hits (excluding disordered and repeated structures, no experimental temperature specification) for which the histograms (Fig. 6) were generated using Vista software. The histograms clearly demonstrate that the coordination Cu–O and Cu–N bonds in **1** and **2** correspond to the frequently reported values.

2.2. Quantum chemical calculations

Geometries obtained from DFT calculations are in good agreement with the XRD data. Overall relaxation of the geometry is observed (Table 2), which can be explained by absence of crystalline intermolecular interactions. For both **1c** and **2c** similar trends in geometry were observed. Geometries of **2** and **2'** arrive in the same true minima (**2c**) on the potential energy surface as revealed by frequency analysis performed for optimized structures. Both optimized structures gained regular square-planar conformation (Table 2). Dihedral angle P_A/P_B arrived to the ideal value of 90.0° . Optimized geometry of **3c** does not arrive to the ideal square-bipyramidal coordination, which can be explained by several intramolecular interactions detected by QTAIM. As suggested by QTAIM calculations Cu–O and Cu–N bonds in all three calculated structures can be classified as dative, intermediate between closed-shell and shared interactions. Dative bonds are characterized by: (1) electron density (ρ) value lying in range 0.050 – 0.150 au, being intermediate between values for ionic and covalent interactions; (2) positive value of the Laplacian of the electron density ($\nabla^2 \rho > 0$); (3) small negative value of the total energy density (H), defined as a sum of kinetic energy density (G), and the potential energy density (V) at the bond critical point (BCP) [7,31]. For **1c**–**3c** the coordination Cu–O(carboxyl) bonds are the strongest as suggested by the ρ_{BCP} values (Table 4). The values of the electron density at the BCPs of Cu–N(Py) are equal to 0.076 and 0.078 $\text{e} \text{Å}^{-3}$ for **1c** and **2c**, respectively, and 0.076 $\text{e} \text{Å}^{-3}$ of Cu–O(H₂O) for **3c** are similar, implying the same strength of these bonds. Noteworthy that metal–dnb and metal–DMSO bonds in **3c** are described with the same ρ_{BCP} value, larger than Cu–N bonds in **1c** and **2c**, suggesting substitution of pyridine with DMSO. No decrease in ρ_{BCP} of Cu–O(carboxyl) was observed upon increasing of the metal coordination number. Topological features of the metal coordination environment are reflected in the geometrical features, the greater values of ρ_{BCP} correspond to the shorter bond lengths. The obtained energy density properties: H , G and V for the dative bonds of **1c**, **2c** and **3c** are in good agreement with the results reported in the literature [32,14]. The absence of bond paths between carbonyl oxygen atoms [O(2) and O(8)] and metal centers confirms the square-planar

geometry of Cu(II) (Fig. 7). Furthermore, QTAIM analysis revealed four intramolecular C–H...O interactions between pyridine and carboxylate residues similar for **1c** and **2c**, which do not obey “geometrical criteria” of hydrogen bonding [29] (CHO angle around 113°). These interactions are described by the presence of BCP, and the bond path that connects CH-donor and O-acceptor atoms. Values of the electron density and Laplacian of the electron density at the BCPs (averaged $\rho_{\text{BCP}} = 0.013(1)$ $\text{e} \text{Å}^{-3}$ and $\nabla^2 \rho_{\text{BCP}} = 0.040(1)$ $\text{e} \text{Å}^{-5}$) lie within normal range of contacts describing hydrogen bonds [33–35] (Table 5), thus bringing further stabilization for metal environment. Due to intramolecular interactions, four nonstructural rings are formed, with values of the electron density at the ring critical points (ρ_{RCP}) twice lower than in benzene and pyridine rings (Table 5). Topological analysis of **3c** supports crystallographic data on intramolecular hydrogen bonding, local density properties of O–H...O bonds are described by: $\rho_{\text{BCP}} = 0.060$ $\text{e} \text{Å}^{-3}$ and $\nabla^2 \rho_{\text{BCP}} = 0.156$ $\text{e} \text{Å}^{-5}$. Due to the mentioned interactions two nonstructural rings are formed: Cu(1)–O(1w)–H(1w)–O(2)–C(1)–O(1) and Cu(1)–O(1w')–H(1w')–O(2')–C(1')–O(1'), with the local density properties: $\rho_{\text{BCP}} = 0.014$ $\text{e} \text{Å}^{-3}$, and $\nabla^2 \rho_{\text{BCP}} = 0.064$ $\text{e} \text{Å}^{-5}$. Other two nonstructural rings are formed because of C–H(DMSO)...O(carboxyl) intramolecular contacts ($\rho_{\text{BCP}} = 0.010$ $\text{e} \text{Å}^{-3}$ and $\nabla^2 \rho_{\text{BCP}} = 0.031$ $\text{e} \text{Å}^{-5}$) described with the drastically decrease of ρ_{RCP} value compared to the benzene rings: 0.003 versus 0.021 $\text{e} \text{Å}^{-3}$, suggesting weak H...O interaction (Table 5).

3. Conclusions

Two novel mononuclear Cu-carboxylate complexes [Cu(H₂-btc)₂(Py)₂] and [Cu(dnb)₂(Py)₂] were obtained by reaction of copper(II) acetate with pyridine (Py) and two similar benzoic acids, benzene-1,3,5-tricarboxylic (H₃-btc), and 3,5-dinitro-benzoic acid (H-dnb) in anhydrous medium. Recrystallization of [Cu(dnb)₂(Py)₂] from DMSO resulted in octahedral complex [Cu(dnb)₂(DMSO)₂(H₂O)₂]. Low temperature single crystal X-ray structural study and topological analysis of the theoretical electron densities according to the quantum theory of atoms in molecules are in agreement for these three complexes. Consideration of a number of local electron density properties at the bond critical points (BCPs) including ρ_{BCP} , $\nabla^2 \rho_{\text{BCP}}$ and total electron energy density H provided insight into metal center environment and stabilizing intramolecular short interactions. The square-planar primary coordination sphere in [Cu(H₂-btc)₂(Py)₂] and [Cu(dnb)₂(Py)₂] is augmented by a long distance with the second O atom of the coordinated carboxylic group which participates in short homomeric H₂-btc...H₂-btc intermolecular contacts in [Cu(H₂-btc)₂(Py)₂], and heteromeric dnb...Py intermolecular contacts in [Cu(dnb)₂(Py)₂] in the crystal. The absence of the bond

paths as revealed by QTAIM between this carbonyl oxygen atom and metal centers confirms the square-planar geometry of Cu(II). Furthermore, QTAIM analysis revealed four intramolecular C–H···O interactions between pyridine rings and carboxylate residues in complexes **1** and **2**, which bring additional stabilization to the metal environment. Topological analysis of octahedral complex [Cu(dnb)₂(DMSO)₂(H₂O)₂] supports crystallographic data on intramolecular hydrogen bonding, and reveals two other nonstructural rings formed because of C–H(DMSO)···O(carboxyl) intramolecular interactions that stabilize the octahedral Cu(II) environment.

Acknowledgments

We thank Prof. T.V. Timofeeva for fruitful discussions. This work was supported by the NSF-DMR grant 0934212. The authors are grateful for this support.

Appendix A. Supplementary data

CCDC 806864, 806865, and 806866 contains the supplementary crystallographic data for this paper. These data can be obtained free of charge via <http://www.ccdc.cam.ac.uk/conts/retrieving.html>, or from the Cambridge Crystallographic Data Centre, 12 Union Road, Cambridge CB2 1EZ, UK; fax: (+44) 1223-336-033; or e-mail: deposit@ccdc.cam.ac.uk.

References

- [1] (a) B.F. Hoskins, R.J. Robson, *Am. Chem. Soc.* 112 (1990) 1546; (b) H. Li, M. Eddaoudi, M. O’Keeffe, O.M. Yaghi, *Nature* 402 (1999) 276; (c) G. Férey, *Chem. Soc. Rev.* 37 (2008) 191.
- [2] S.V. Kolotuchin, E.E. Fenlon, S.R. Wilson, C.J. Loweth, S.C. Zimmerman, *Angew. Chem., Int. Ed.* 34 (1996) 2654.
- [3] S.S.-Y. Chui, S.M.-F. Lo, J.P.H. Charmant, A.G. Orpen, I.D. Williams, *Science* 283 (5405) (1999) 1148.
- [4] (a) Y. Wu, A. Kobayashi, G.J. Halder, V.K. Peterson, K.W. Chapman, N. Lock, P.D. Southon, C.J. Kepert, *Angew. Chem., Int. Ed.* 47 (2008) 8929; (b) R. Pech, J. Pickardt, *Acta Crystallogr., Sect. C* 44 (1988) 992; (c) K.E. Holmes, P.F. Kelly, M.R.J. Elsegood, *Dalton Trans.* (2004) 3488; (d) L. Yang, H. Naruke, T. Yamase, *Inorg. Chem. Commun.* 6 (2003) 1020; (e) Q.-W. Zhang, G.-X. Wang, *Z. Kristallogr.-New Cryst. Struct.* 221 (2006) 101; (f) C.-Y. Sun, S.-X. Liu, D.-D. Liang, K.-Z. Shao, Y.-H. Ren, Z.-M. Su, *J. Am. Chem. Soc.* 131 (2009) 1883.
- [5] (a) W. Li, M.-X. Li, J.-J. Yang, M. Shao, H.-J. Liu, *J. Coord. Chem.* 61 (2008) 2715; (b) X.-L. Wang, H.-Y. Lin, G.-C. Liu, H.-Y. Zhao, B.-K. Chen, *J. Organomet. Chem.* 693 (2008) 2767; (c) M.-L. Hu, Q. Shi, H.-P. Xiao, Fan Chen, *Z. Kristallogr.-New Cryst. Struct.* 219 (2004) 17; (d) G.-B. Che, C.-B. Liu, B. Liu, Q.-W. Wang, Z.-L. Xu, *Cryst. Eng. Commun.* 10 (2008) 184; (e) P. Wang, C.N. Moorefield, M. Panzer, G.R. Newkome, *Chem. Commun.* (2005) 465; (f) W. Li, M.-X. Li, M. Shao, Z.-X. Wang, H.-J. Liu, *Inorg. Chem. Commun.* 11 (2008) 954; (g) J. Yang, J.-F. Ma, Y.-Y. Liu, J.-C. Ma, H.-Q. Jia, N.-H. Hu, *Eur. J. Inorg. Chem.* (2006) 1208; (h) M. Du, Z.-H. Zhang, Y.-P. You, X.-J. Zhao, *Cryst. Eng. Commun.* 10 (2008) 306; (i) L.-P. Zhang, J. Yang, J.-F. Ma, Z.-F. Jia, Y.-P. Xie, G.-H. Wei, *Cryst. Eng. Commun.* 10 (2008) 1410; (j) F. Luo, J. Min Zheng, S.R. Batten, *Chem. Commun.* (2007) 3744.
- [6] (a) C.D. Ene, F. Tuna, O. Fabelo, C. Ruiz-Perez, A.M. Madalan, H.W. Roesky, M. Andruh, *Polyhedron* 27 (2008) 574; (b) H. Abourahma, B. Moulton, V. Kravtsov, M.J. Zaworotko, *J. Am. Chem. Soc.* 124 (2002) 9990; (c) X.-J. Li, R. Cao, Z.-G. Guo, Y.-F. Li, X.-D. Zhu, *Polyhedron* 26 (2007) 3911; (d) P. Stachova, M. Korabik, M. Koman, M. Melnik, J. Mrozinski, T. Glowiak, M. Mazur, D. Valigura, *Inorg. Chim. Acta* 359 (2006) 1275; (e) H.-J. Chen, J. Zhang, W.-L. Feng, M. Fu, *Inorg. Chem. Commun.* 9 (2006) 300; (f) A.D. Burrows, C.G. Frost, M.F. Mahon, M. Winsper, C. Richardson, J.P. Attfield, J.A. Rodgers, *Dalton Trans.* (2008) 6788.
- [7] R.F.W. Bader, *Atoms in Molecules – A Quantum Theory*, Oxford University Press, Oxford, 1990.
- [8] C.F. Matta, R.J. Boyd (Eds.), *The Quantum Theory of Atoms in Molecules*, Wiley-VCH, Weinheim, 2007.
- [9] C.L. Firme, D.deL. Pontesa, O.A.C. Antunes, *Chem. Phys. Lett.* 499 (2010) 193.
- [10] (a) I. Cukrowski, C.F. Matta, *Chem. Phys. Lett.* 499 (2010) 66; (b) I. Cukrowski, K.K. Govender, *Inorg. Chem.* 49 (2010) 6931.
- [11] F. Wieseemann, S. Teipel, B. Krebs, U. Hoeweler, *Inorg. Chem.* 33 (1994) 1891.
- [12] P. Coppens, B. Iversen, F.K. Larsen, *Coord. Chem. Rev.* 249 (2005) 179.
- [13] L.J. Farrugia, D.S. Middlemiss, R. Sillanp, P. Sepp, *J. Phys. Chem. A* 112 (2008) 9050.
- [14] A. Robertazzi, A. Magistrato, P. De Hoog, P. Carloni, J. Reedijk, *Inorg. Chem.* 46 (2007) 5873.
- [15] E.B. Miminoshvili, K.E. Miminoshvili, G.P. Adeishvili, *Zh. Strukt. Khim. (Russ.) J. Struct. Chem.* 47 (2006) 95.
- [16] K. Bania, N. Baroah, R. Sarma, J.B. Baruah, *J. Chem. Cryst.* 38 (2008) 57.
- [17] SADABS, Bruker Analytical X-ray System, Inc., Madison, WI, 1999.
- [18] A.L. Spek, *J. Appl. Crystallogr.* 36 (2003) 7.
- [19] (a) SAINT+, Version 6.2a, Bruker Analytical X-ray System, Inc., Madison, WI, 2001.; (b) SHELXTL, Version 6.10, Bruker Analytical X-ray System, Inc., Madison, WI, 1997.
- [20] M.J. Frisch, G.W. Trucks, H.B. Schlegel, G.E. Scuseria, M.A. Robb, J.R. Cheeseman, G. Scalmani, V. Barone, B. Mennucci, G.A. Petersson, H. Nakatsuji, M. Caricato, X. Li, H.P. Hratchian, A.F. Izmaylov, J. Bloino, G. Zheng, J.L. Sonnenberg, M. Hada, M. Ehara, K. Toyota, R. Fukuda, J. Hasegawa, M. Ishida, T. Nakajima, Y. Honda, O. Kitao, H. Nakai, T. Vreven, J.A. Montgomery, Jr., J.E. Peralta, F. Ogliaro, M. Bearpark, J.J. Heyd, E. Brothers, K.N. Kudin, V.N. Staroverov, R. Kobayashi, J. Normand, K. Raghavachari, A. Rendell, J.C. Burant, S.S. Iyengar, J. Tomasi, M. Cossi, N. Rega, J.M. Millam, M. Klene, J.E. Knox, J.B. Cross, V. Bakken, C. Adamo, J. Jaramillo, R. Gomperts, R.E. Stratmann, O. Yazyev, A.J. Austin, R. Cammi, C. Pomelli, J.W. Ochterski, R.L. Martin, K. Morokuma, V.G. Zakrzewski, G.A. Voth, P. Salvador, J.J. Dannenberg, S. Dapprich, A.D. Daniels, O. Farkas, J.B. Foresman, J.V. Ortiz, J. Cioslowski, D.J. Fox, *GAUSSIAN09, Revision A.02*, Gaussian, Inc., Wallingford CT, 2009.
- [21] A.D. Becke, *J. Chem. Phys.* 98 (1993) 5648.
- [22] C. Lee, W. Yang, R.G. Parr, *Phys. Rev. B* 37 (1988) 785.
- [23] S.H. Vosko, L. Wilk, M. Nusair, *Can. J. Phys.* 58 (1980) 1200.
- [24] P.J. Hay, W.R. Wadt, *J. Chem. Phys.* 82 (1985) 270.
- [25] Todd A. Keith, AIMAll (Version 10.12.08), 2010 (aim.tkgristmill.com).
- [26] (a) D.E. Lynch, *Acta Crystallogr., Sect. E* 58 (2002) m577; (b) M.-L. Hu, Q. Shi, H.-P. Xiao, F. Chen, Z. Kristallogr.-New Cryst. Struct. 219 (2004) 17; (c) M.D. Stephenson, M.J. Hardie, *Dalton Trans.* (2006) 3407; (d) Q.-L. Wang, C.-Z. Xie, D.-Z. Liao, S.-P. Yan, Z.-H. Jiang, P. Cheng, *Transition Met. Chem.* 28 (2003) 16.
- [27] M.C. Etter, *Acc. Chem. Res.* 23 (1990) 120.
- [28] J.-W. Ye, D. Li, K.-Q. Ye, Y. Liu, Y.-F. Zhao, P. Zhang, *Z. Anorg. Allg. Chem.* 634 (2008) 345.
- [29] G.R. Desiraju, T. Steiner, *The Weak Hydrogen Bond: In Structural Chemistry and Biology*, Oxford University Press, USA, 2001.
- [30] F.N. Allen, *Acta Crystallogr., Sect. B* 58 (2002) 380.
- [31] P. Macchi, A. Sironi, *Coord. Chem. Rev.* 238/239 (2003) 383.
- [32] F. Hueso-Ureña, S.B. Jiménez-Pulido, M.P. Fernández-Liencres, M. Fernández-Gómez, M.N. Moreno-Carretero, *Dalton Trans.* 2008 (2008) 6461.
- [33] U. Koch, P.L.A. Popelier, *J. Phys. Chem. A* 99 (1995) 9747.
- [34] P. Popelier, *Atoms in Molecules. An Introduction*, Prentice-Hall, Englewood Cliffs, NJ, 2000.
- [35] S.J. Grabowski, *J. Phys. Org. Chem.* 17 (2004) 18.